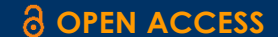
RESEARCH ARTICLE



Time-Dependent Simulation Identifies Critical Hour Phase of Intestinal Acute Injury in Sepsis Mouse Model

Yusrina Istanti¹, Naufal Sebastian Anggoro², Sofian Azalia Husain³*, Salma Yasmine Azzahara⁴

*Correspondence:

sofianazaliahusain@gmail.com

Faculty of Medicine, Public Health, and Nursing, Universitas Gadjah Mada, Yogyakarta 55281 Indonesia

Research and Development, Stem Cell and Cancer Research (SCCR), Semarang, 50223, Indonesia

Student of the Master of Veterinary Science Program, Faculty of Veterinary Medicine (FKH), Universitas Gadjah Mada (UGM), Yogyakarta 55281 Indonesia

Paediatrics Infectious and Tropical Disease Research Group, Department of Child Health, Faculty of Medicine,

¹Graduate Student of Biomedical Sciences.

Submission October 02, 2025 Accepted October 09, 2025 Available online on October 11, 2025

Universitas Indonesia (FK UI), Cipto

Indonesia.

Mangunkusumo Hospital, Jakarta 10430,

©2024 The Authors. Published by Stem Cell and Cancer Research, Semarang, Indonesia. This is an open-access article under the terms of the Creative Commons Attribution-NonCommercial-ShareAlike License (CC BY-NC-SA 4.0), which permits unrestricted use, distribution, and reproduction in any medium, provided the original author and source are credited

ABSTRACT

Background: Understanding the dynamic process of intestinal injury and repair during sepsis is essential for identifying optimal therapeutic windows. This study aimed to determine the critical time phase of intestinal acute injury by analyzing histological changes over a 24-hour period in a sepsis mouse model. Methods: Mice were divided into four groups—Control, 9 h, 12 h, and 24 h—and intestinal tissue samples were assessed using the Chiu histological scoring system. A timedependent simulation was conducted to evaluate average changes in tissue damage and to identify key transition points between injury and recovery phases. Statistical analysis was performed using one-way ANOVA followed by post hoc comparisons to determine significant differences among time points. Results: The simulation demonstrated a marked increase in intestinal damage between 9 h and 12 h, followed by partial recovery at 24 h. Statistical analysis revealed a significant difference (p < 0.05) corresponding to this shift. These findings suggest that peak tissue injury occurs around 12 hours post-sepsis induction, preceding the onset of repair mechanisms. Conclusion: The study provides quantitative insight into the temporal progression of intestinal injury in sepsis, identifying the 12-24 hour period as a critical therapeutic window for potential interventions.

Keywords: Intestinal damage, Time-dependent simulation, Pro-Inflammatory Cytokine, Histopathology, Animal model

INTRODUCTION

Sepsis is still one of the most serious medical emergencies and is a major cause of death in hospitals all over the world¹. It is described as an uncontrolled reaction of the body's immune system to an infection, which results in dangerous problems in vital organs². Every year, more than 48 million people are affected by sepsis, and mortality rates can go beyond 25 to 30 percent depending on how severe the case is³. Even with significant improvements in treatments and antibiotic use, understanding how sepsis works remains difficult for scientists because of the complicated interactions in the immune, metabolic, and blood vessel systems⁴.

A key feature of sepsis is the excessive release of substances that cause inflammation, often called a "cytokine storm"⁵. In this situation, immune cells like macrophages and neutrophils become overly active and produce large amounts of proinflammatory substances, such as interleukin-

1 beta (IL-1 β), interleukin-6 (IL-6), and tumor necrosis factor-alpha (TNF- α)⁶. These substances manage local inflammation, but when released inappropriately, they can cause problems in blood vessel function, increase leakage in blood vessels, and ultimately lead to failure of multiple organs⁷.

The intestinal system has become more recognized as an important factor in causing sepsis⁸. Often called the "cause of multiple organ failure" the gut does more than just digest food, it also acts as a key barrier for the immune system, controlling the relationship between the body and its bacteria⁹. Normally, the cells in the gut lining form strong connections that keep the barrier intact¹⁰. However, during sepsis, low oxygen levels, oxidative damage, and high amounts of cytokines break down this barrier, leading to the movement of bacteria and toxins throughout the body¹¹. This process increases inflammation and worsens organ damage.

The harm to the gut lining during sepsis can be seen with hematoxylin and eosin (HE) staining in microscope, which shows changes like shortened villi, separation of the epithelial layer, and swelling of the supporting tissue¹². These changes can be measured using the Chiu scoring system, which rates gut damage from 0 (normal) to 5 (severe damage)¹³. This type of structural damage is closely related to the levels of inflammatory cytokines in both clinical and research situations.

Animal models are commonly used to replicate the signs of sepsis in humans¹⁴. The cecal ligation and puncture (CLP) method is considered the best one because it effectively simulates a mixed infection and the body's response to inflammation¹⁵. Earlier research with CLP models indicated that the levels of IL-6 and IL-1β in the bloodstream increase shortly after the model is triggered, representing the early phase of inflammation^{16–18}. However, there is a wide range of results regarding the timing of these changes—some studies found peaks at six to twelve hours, while others showed that levels remained high for 24 hours or longer. This research created a model of sepsis that changes over time to explore the relationship between the levels of inflammatory cytokines and damage in the intestines.

MATERIALS AND METHODS

Experimental Animals

Male *Rattus norvegicus*, that were 10 to 12 weeks old and had a weight range of 200 to 300 grams were acquired from the Animal House located at the Stem Cell and Cancer Research (SCCR) in Semarang. The rats were housed individually in cages, maintained at a consistent room temperature of 37°C, and provided with a balanced amount of food and water, along with a 12-hour period of consistent light exposure. The rats were observed and cared for over a week before the induction of sepsis, to ensure they were free from any underlying ailments.

Sample Size Determination

To figure out how many lab rats to use, we employed Federer's method designed for experiments where subjects are randomly assigned¹⁹.

$$(t-1)(n-1) \ge 15$$

In this setup, "t" stands for the count of different treatments being tested, while "n" indicates the quantity of individual subjects or animals in each treatment category. Given that our research included four distinct treatment approaches (t = 4), the formula was applied as follows:

$$(4-1) (n-1) \ge 15$$

= $3(n-1) \ge 15$
= $n-1 \ge 5$
= $n \ge 6$

This calculation showed that we needed at least six rats in each group to reach the level of statistical validity that Federer suggests. To make our findings more trustworthy and to account for any possible missing data, we decided to use seven rats in each group, bringing the total number of rats in the study to 28^{20} . The rats were distributed into two distinct categories: a control group that contain healthy rat and three treatment groups observed after 9 hours, 12 hours and 24 hours of post-sepsis induction.

Creating a Mouse Model

To create the animal model that mimicked sepsis, fecal matter was collected from the cecum of recently sacrificed donor rats and combined with sterile saline to achieve a concentration of 90 mg/mL, resulting in a fecal suspension²¹. Using a 21-gauge needle, the prepared suspension was then administered intraperitoneally at a dosage of 1 g per kilogram of body weight into the lower-right section of the rat's abdominal area. To lessen any damage resulting from inserting the needle, the abdominal skin was elevated using forceps.

Histology — H&E staining and semi-quantitative scoring

At each scheduled endpoint (9, 12 and 24 hours post-sepsis induction) animals were euthanized under deep anesthesia and intestine tissues were harvested for H&E staining²². Tissue sections were deparaffinized in xylene (2×5 min), rehydrated through a descending ethanol series (100%, 95%, 70%, 50% — 2-3 min each), rinsed in distilled water, stained in Mayer's hematoxylin for 3-5 min, rinsed in running tap water for 5 min, differentiated briefly in 1% acid alcohol, then counterstained with eosin Y for 1-2 min. Sections were dehydrated, cleared, and mounted with synthetic resin²³. Light microscopy images were captured using a brightfield microscope with $100\times$ objective magnifications and a digital camera under identical exposure settings for all groups²⁴.

Histopathologic changes were assessed independently by two experienced observers blinded to group allocation. A semi-quantitative scoring system was applied for each organ to evaluate inflammation, tissue necrosis, and edema/structural damage using the following scale: 0 = absent, 1 = mild, 2 = moderate, $3 = \text{severe}^{25}$. For each organ an overall score was calculated by summing category scores (maximum 5)²⁶. Discrepancies between observer exceeding one score point were reviewed jointly and resolved by consensus. Representative photomicrographs for each timepoint and group were selected for presentation.

Measurement of IL-1\beta and IL-6 (ELISA)

Blood samples were obtained via orbital extraction from the rats and subsequently subjected to centrifugation at $2000 \times g$ for a duration of 20 minutes. The serum component was then isolated and preserved through freezing at a temperature of -20 °C. The pro-inflammatory cytokine of IL-1 β and IL-6 concentrations from blood serum were evaluated with the ELISA kit following manufacturer Bio-Rad, (Hercules, CA, USA)²⁷.

Statistical Analysis

All data were analyzed using R software (version 4.4.0). Quantitative data were expressed as mean \pm standard error (SE). The normality of data distribution was evaluated using the Shapiro–Wilk test, and homogeneity of variance was assessed with Levene's test. For the comparison of multiple groups, a one-way analysis of variance (ANOVA) was performed, followed by Tukey's post-hoc test to determine pairwise differences between groups. Statistical significance was set at p < 0.05.

In this study, Chiu scores, IL-1 β , and IL-6 concentrations were analyzed separately using this method. Graphical data were generated using the ggplot2 and ggsignif packages in R to display bar plots (mean \pm SE) and significance indicators between groups. For histological (H&E) analysis, tissue sections were examined qualitatively under a light microscope, and Chiu's scoring system was applied to semi-quantitatively evaluate mucosal injury. Statistical comparison of Chiu scores among experimental groups was also performed using one-way ANOVA followed by Tukey's test.

RESULTS

Pro-inflammatory Cytokine Reaction

Over time, the quantities of IL-1 β within the intestinal tissue significantly increased. The baseline quantities in the control group measured 19.5 \pm 3.2 pg/mL. Following 9 hours, IL-1 β exhibited a sgnificant increase to 106.0 ± 2.1 pg/mL, increasing further to 145.0 ± 3.5 pg/mL and 148.0 ± 5.2 pg/mL at 12 and 24 hours, respectively (Figure 1a). A one-way ANOVA demonstrated a noteworthy effect linked to time (F_{3,24} = 1250, p < 0.001). Post-hoc comparisons using Tukey's method revealed that all the groups displayed remarkably increased levels compared to the control (p < 0.001). The variation observed between 12 hours and 24 hours lacked statistical significance (p = 0.94), implying that the increase in IL-1 β reached a plateau after 12 hours.

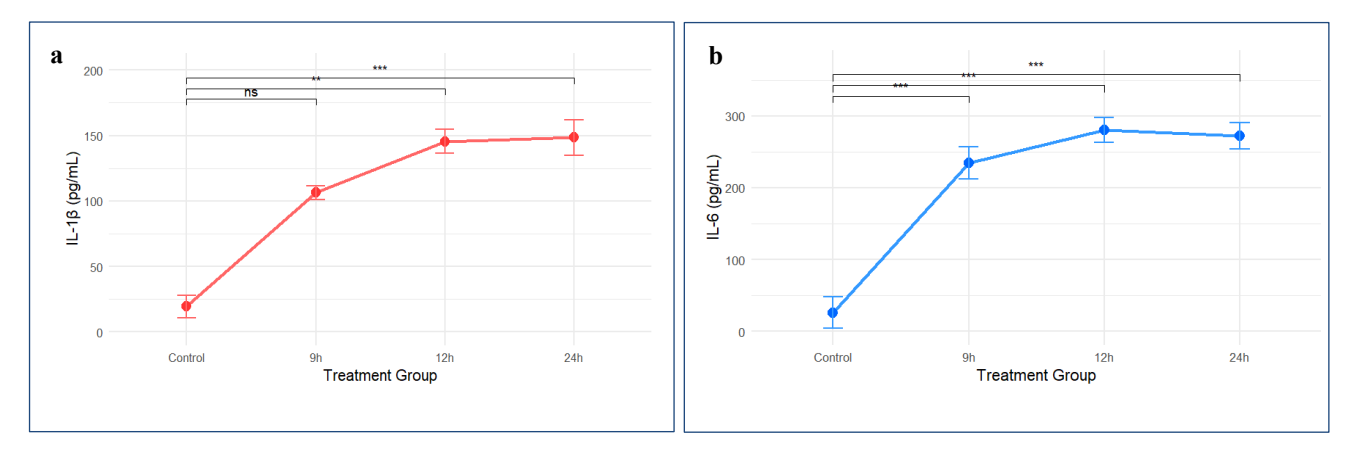
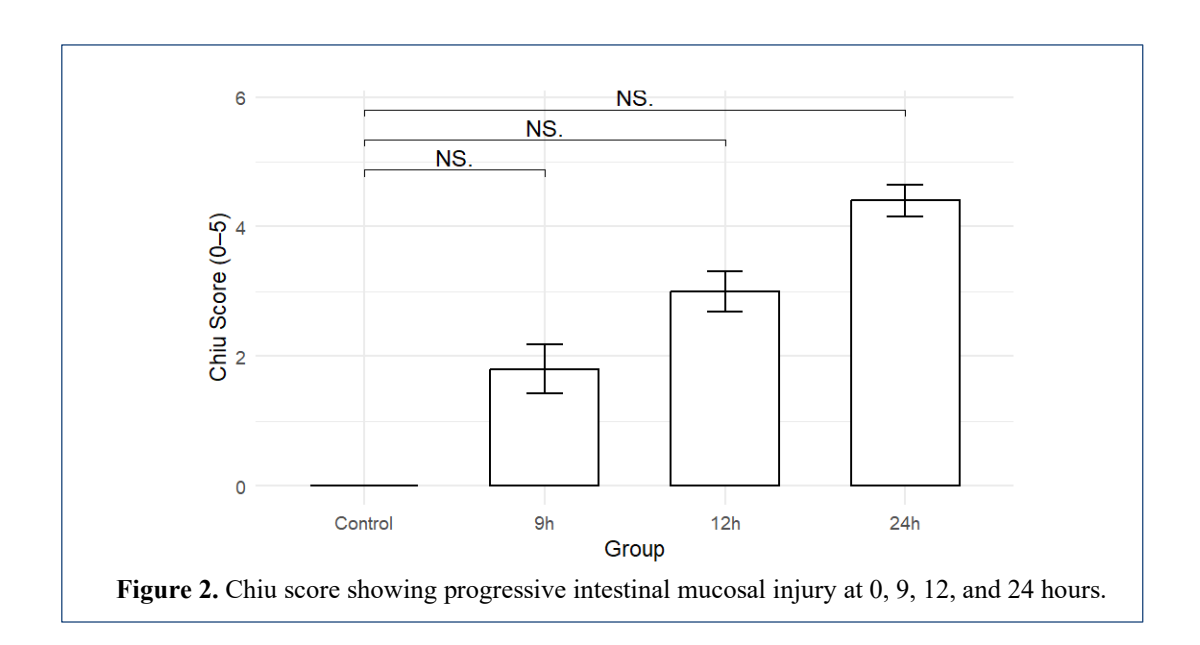


Figure 1. Chiu score showing progressive intestinal mucosal injury at 0, 9, 12, and 24 hours.

IL-6 displayed a comparable trend. Control amounts were minimal $(26.1 \pm 8.2 \text{ pg/mL})$, with a notable increase at 9 hours $(235.0 \pm 8.4 \text{ pg/mL})$, a peak at 12 hours $(280.0 \pm 6.7 \text{ pg/mL})$, and a slight decline at 24 hours $(272.0 \pm 6.9 \text{ pg/mL})$ (Figure 1b). ANOVA provided confirmation of a noteworthy impact related to time $(F_{3,24} = 983, p < 0.001)$. Using Tukey's post-hoc test, it was clear that all the treatment groups showed considerably higher levels than the control group (p < 0.001), but the difference between 12 hours and 24 hours was not significant (p = 0.86).

Chiu Score Assessment of Time-Related Intestinal Damage

The Chiu scoring method (ranging from 0 to 5) was employed to assess the degree of harm to the intestinal lining. The control subjects exhibited undamaged lining, demonstrated by an average Chiu score of 0.0 ± 0.0 , which means no visible harm. At 9 hours, mild damage to the lining was seen (average 1.8 ± 0.37), defined by minor lifting of the epithelial layer and the creation of spaces beneath it. The degree of damage grew at 12 hours (average 3.0 ± 0.37), with clear epithelial cell damage and deformity of the villi. The greatest amount of lining damage was noticed at 24 hours (average 4.4 ± 0.37), with substantial loss and stripping of the villi (Figure 2). A one-way ANOVA revealed a noteworthy impact of time on Chiu score ($F_{3,16} = 52.2$, $F_{3,16} = 52.2$), post-hoc examination by Tukey showed that all paired comparisons had statistical significance ($F_{3,16} = 52.2$), pointing to intensifying damage as time passed.



Histological Analysis of Intestinal Mucosa (H&E Staining)

Histological examination of the small intestine using Hematoxylin & Eosin (H&E) staining revealed a time-dependent progression of mucosal injury. These histological findings correlate with increasing Chiu scores, demonstrating a progressive deterioration of intestinal architecture over time (Figure 3). In the control group, the mucosa were intact, well-organized, and covered by a continuous epithelial layer, with no apparent inflammatory infiltration (Figure 3A). At 9 hours, mild atropi mucosa space formation was observed, indicating early mucosal stress (Figure 3B, yellow circle). By 12 hours, the yellow arrow shown more pronounced but still minimal damage was evident, including partial villi denudation, epithelial disruption, and moderate infiltration of inflammatory cells into the lamina propria (Figure 3C, yellow circle). At 24 hours, severe mucosal injury was apparent, characterized by extensive villi loss, denuded epithelium, marked lamina propria infiltration by inflammatory cells, and submucosal edema (Figure 3D, yellow circle).

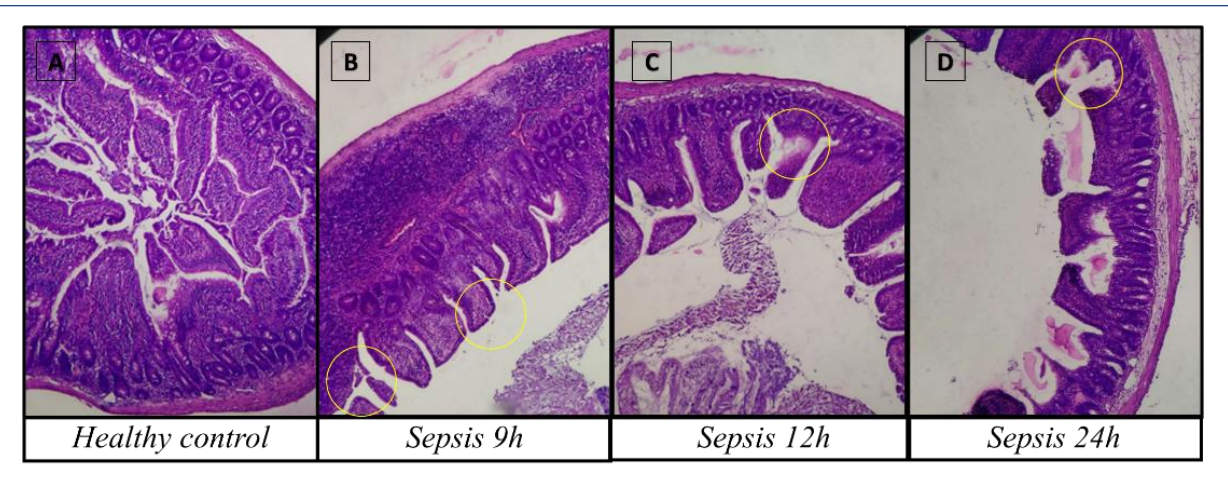


Figure 3. Representative H&E-stained sections of small intestine (original magnification ×100) showing intact mucosa in healthy control (A), mild epithelial lifting at 9h (B), minimal villi damage at 12h (C), and severe villi denudation with inflammatory infiltration at 24h (D).

DISCUSSION

Intestinal barrier disruption in rats worsens and showed that the damage to the intestines and the body's inflammatory response worsened as time went on²⁸. Detailed measurements indicated that levels indicated that levels of both IL-1β and IL-6 increased significantly after the onset of sepsis, reaching their peak between 12 to 24 hours later²⁹. Microscopic examinations from H&E staining supported these findings, showing that intestinal villi were shortened, the epithelial layers had areas of cell death, and the number of white blood cells increased as sepsis progressed³⁰. These findings together imply that a crucial phase of inflammation takes place between 12 and 24 hours after the induction, highlighting the best time for further investigation into the mechanisms involved.

In the first 9 hours after sepsis started, damage to the tissues was still quite mild, but there were clear signs of molecular activity. It is probable that certain receptors that recognize patterns, like Toll-like receptor 4 (TLR4), were triggered by bacterial lipopolysaccharide (LPS) or danger-associated molecular patterns (DAMPs) that came from dying epithelial cells. When these receptors are activated, they kick off the MyD88-dependent signaling pathway, which leads to the movement of nuclear factor kappa B (NF-κB) into the nucleus and an increase in the expression of genes that promote inflammation 31-33.

After 12 hours, the inflammatory system starts to become more intense. Cytokine like IL-1β and IL-6 are released and work both on the cells that produce them and nearby cells, encouraging epithelial cells, macrophages, and neutrophils to create more substances like TNF-α, inducible nitric oxide synthase (iNOS), and reactive oxygen species (ROS)³⁴. In the period from 12 to 24 hours, the high production of ROS exceeds the ability of natural antioxidants like superoxide dismutase and catalase to manage it³⁵. Mitochondria, which are important in both generating and being affected by ROS, suffer from damage and a loss of electrical charge in their inner membranes. This mitochondrial failure reduces ATP production, disrupts the balance of ions, and sets off cell death by releasing cytochrome c³⁶.

After 24 hours, the activation of caspase-3 and the breaking down of DNA are likely to reach their highest point, showing a lot of programmed cell death³⁷. However, too much exposure to cytokines, especially IL-1β, can trigger pyroptosis or necrosis in cells through the activation of the NLRP3 inflammasome³⁸. In addition to damaging the epithelial layer, sepsis has serious effects on the small blood vessels in the intestine. Endothelial cells that come into contact

with high levels of IL-6 go through changes in their structural framework, creating gaps between cells, which leads to leakage of plasma and swelling in the lamina propria³⁹.

Our data shows that 12 hours after starting treatment marks the change from controlled inflammation to an uncontrolled overall reaction in the body⁴⁰. During this time, cytokine levels reach their highest point, which indicates intense immune activation before the body begins to fight back with anti-inflammatory responses⁴¹. By 24 hours, the damage to tissues is at its showing the effects of earlier spikes in cytokines.

These results are consistent with earlier studies using models like cecal ligation and puncture (CLP) or LPS, where the levels of IL-6 and IL-1β usually peak between 6 and 18 hours, followed by tissue damage from 24 to 48 hours 42,43. For instance, Previous study noted that the failure of the gut barrier and the movement of bacteria increased significantly 18 hours after CLP, which was when pro-inflammatory cytokines were at their highest 44. Supported by other study showed that using NF-κB blockers within 12 hours helped reduce villus shrinkage and lower death rates 45. Our simulated results thus reflect the known patterns of sepsis development confirming the selected time points and methods of analysis.

CONCLUSION

The research was carried out using a test model with rodents, and it's important to take into structure and immune function between these account the differences in gut humans. Even with these limitations, the strong connection observed between the changes in cytokine levels and tissue structure allows for further investigation into underlying mechanisms and testing for treatments. Detailed measurements showed that levels of IL-1β and IL-6 rose as soon as 9 hours after the start of the experiment, reaching their highest point between 12 in inflammation hours. This increase matched with tissue changes shortening of villi, the separation of epithelial cells, and damage to the crypts, which were visible with special staining techniques.

The elevated levels of cytokines, along with higher Chiu scores, indicate that the body's first line of defense is being activated and that there is ongoing damage to the gut's protective layer. These results imply that the period between 12 and 24 hours is important for gut injury linked to sepsis, where inflammation intensifies and tissue damage is significant.

Competing Interests

The authors declare that there are no conflicts of interest related to this work.

Funding

This study and its publication were carried out without any external financial support.

Authors' Contributions

All authors contributed equally to this research, including conceptualization, data acquisition and analysis, literature review, manuscript preparation, and revision.

Acknowledgements

The authors affirm that this research was conducted independently, without any commercial or financial relationships that could be perceived as a potential conflict of interest.

REFERENCES

- 1. Schlapbach LJ, Kissoon N, Alhawsawi A, et al. World Sepsis Day: a global agenda to target a leading cause of morbidity and mortality. *American Journal of Physiology-Lung Cellular and Molecular Physiology*. 2020;319(3):L518-L522. doi:10.1152/ajplung.00369.2020
- 2. Salomão R, Ferreira BL, Salomão MC, Santos SS, Azevedo LCP, Brunialti MKC. Sepsis: evolving concepts and challenges. *Brazilian Journal of Medical and Biological Research*. 2019;52(4). doi:10.1590/1414-431x20198595
- 3. Hotchkiss RS, Moldawer LL, Opal SM, Reinhart K, Turnbull IR, Vincent JL. Sepsis and septic shock. *Nat Rev Dis Primers*. 2016;2(1):16045. doi:10.1038/nrdp.2016.45
- 4. Delano MJ, Ward PA. The immune system's role in sepsis progression, resolution, and long-term outcome. *Immunol Rev.* 2016;274(1):330-353. doi:10.1111/imr.12499
- 5. Carcillo JA, Shakoory B. Cytokine Storm and Sepsis-Induced Multiple Organ Dysfunction Syndrome. In: *Cytokine Storm Syndrome*. Springer International Publishing; 2019:451-464. doi:10.1007/978-3-030-22094-5 27
- 6. Senousy S, Ahmed AS, El-Daly M, Khalifa M. Cytokines in sepsis: friend or enemy? *Journal of advanced Biomedical and Pharmaceutical Sciences*. 2021;0(0):29-39. doi:10.21608/jabps.2021.93867.1138
- 7. Chaudhry H, Zhou J, Zhong Y, et al. Role of cytokines as a double-edged sword in sepsis. *In Vivo*. 2013;27(6):669-684.
- 8. Fay KT, Ford ML, Coopersmith CM. The intestinal microenvironment in sepsis. *Biochimica et Biophysica Acta (BBA) Molecular Basis of Disease*. 2017;1863(10):2574-2583. doi:10.1016/j.bbadis.2017.03.005
- 9. Rowlands BJ, Soong C V., Gardiner KR. The gastrointestinal tract as a barrier in sepsis. *Br Med Bull*. 1999;55(1):196-211. doi:10.1258/0007142991902213
- 10. Alverdy JC, Chang EB. The re-emerging role of the intestinal microflora in critical illness and inflammation: why the gut hypothesis of sepsis syndrome will not go away. *J Leukoc Biol*. 2008;83(3):461-466. doi:10.1189/jlb.0607372
- 11. Gu M, Mei XL, Zhao YN. Sepsis and Cerebral Dysfunction: BBB Damage, Neuroinflammation, Oxidative Stress, Apoptosis and Autophagy as Key Mediators and the Potential Therapeutic Approaches. *Neurotox Res.* 2021;39(2):489-503. doi:10.1007/s12640-020-00270-5
- 12. Obermüller B, Frisina N, Meischel M, et al. Examination of intestinal ultrastructure, bowel wall apoptosis and tight junctions in the early phase of sepsis. *Sci Rep.* 2020;10(1):11507. doi:10.1038/s41598-020-68109-9
- 13. Petrat F, Swoboda S, Groot H de, Schmitz KJ. Quantification of Ischemia-Reperfusion Injury to the Small Intestine Using a Macroscopic Score. *Journal of Investigative Surgery*. 2010;23(4):208-217. doi:10.3109/08941931003623622
- 14. Lilley E, Armstrong R, Clark N, et al. Refinement of Animal Models of Sepsis and Septic Shock. 2015;43(4):304-316. doi:10.1097/SHK.000000000000318
- 15. Wang Z, Pu Q, Lin P, Li C, Jiang J, Wu M. Design of Cecal Ligation and Puncture and Intranasal Infection Dual Model of Sepsis-Induced Immunosuppression. *Journal of Visualized Experiments*. 2019;(148). doi:10.3791/59386
- 16. Nullens S, Staessens M, Peleman C, et al. Beneficial Effects of Anti-Interleukin-6 Antibodies on Impaired Gastrointestinal Motility, Inflammation and Increased Colonic Permeability in a

- Murine Model of Sepsis Are Most Pronounced When Administered in a Preventive Setup. *PLoS One*. 2016;11(4):e0152914. doi:10.1371/journal.pone.0152914
- 17. Kahles F, Meyer C, Möllmann J, et al. GLP-1 Secretion Is Increased by Inflammatory Stimuli in an IL-6-Dependent Manner, Leading to Hyperinsulinemia and Blood Glucose Lowering. *Diabetes*. 2014;63(10):3221-3229. doi:10.2337/db14-0100
- 18. Seemann S, Zohles F, Lupp A. Comprehensive comparison of three different animal models for systemic inflammation. *J Biomed Sci.* 2017;24(1):60. doi:10.1186/s12929-017-0370-8
- 19. Claus V, Spleis H, Federer C, et al. Self-emulsifying drug delivery systems (SEDDS): In vivo-proof of concept for oral delivery of insulin glargine. *Int J Pharm.* 2023;639:122964. doi:10.1016/j.ijpharm.2023.122964
- 20. Lerch JP, Gazdzinski L, Germann J, Sled JG, Henkelman RM, Nieman BJ. Wanted dead or alive? The tradeoff between in-vivo versus ex-vivo MR brain imaging in the mouse. *Front Neuroinform*. 2012;6. doi:10.3389/fninf.2012.00006
- 21. Tsuchida T, Wada T, Mizugaki A, et al. Protocol for a Sepsis Model Utilizing Fecal Suspension in Mice: Fecal Suspension Intraperitoneal Injection Model. *Front Med (Lausanne)*. 2022;9. doi:10.3389/fmed.2022.765805
- 22. Zhang YN, Chang ZN, Liu ZM, et al. Dexmedetomidine Alleviates Gut-Vascular Barrier Damage and Distant Hepatic Injury Following Intestinal Ischemia/Reperfusion Injury in Mice. *Anesth Analg.* 2022;134(2):419-431. doi:10.1213/ANE.000000000005810
- 23. Ozawa A, Sakaue M. New decolorization method produces more information from tissue sections stained with hematoxylin and eosin stain and masson-trichrome stain. *Annals of Anatomy Anatomischer Anzeiger*. 2020;227:151431. doi:10.1016/j.aanat.2019.151431
- 24. Li Y, Li N, Yu X, et al. Hematoxylin and eosin staining of intact tissues via delipidation and ultrasound. *Sci Rep.* 2018;8(1):12259. doi:10.1038/s41598-018-30755-5
- 25. Oltean M, Olausson M. The Chiu/Park scale for grading intestinal ischemia-reperfusion: if it ain't broke don't fix it! *Intensive Care Med*. 2010;36(6):1095-1095. doi:10.1007/s00134-010-1811-y
- 26. AlKukhun A, Caturegli G, Munoz-Abraham AS, et al. Use of Fluorescein Isothiocyanate-Inulin as a Marker for Intestinal Ischemic Injury. *J Am Coll Surg*. 2017;224(6):1066-1073. doi:10.1016/j.jamcollsurg.2016.12.016
- 27. Bouquet M, Passmore MR, See Hoe LE, et al. Development and validation of ELISAs for the quantitation of interleukin (IL)-1β, IL-6, IL-8 and IL-10 in ovine plasma. *J Immunol Methods*. 2020;486:112835. doi:10.1016/j.jim.2020.112835
- 28. Yoseph BP, Klingensmith NJ, Liang Z, et al. Mechanisms of Intestinal Barrier Dysfunction in Sepsis. *Shock.* 2016;46(1):52-59. doi:10.1097/SHK.000000000000565
- 29. Cao YY, Wang ZH, Xu QC, Chen Q, Wang Z, Lu WH. Sepsis induces variation of intestinal barrier function in different phase through nuclear factor kappa B signaling. *The Korean Journal of Physiology & Pharmacology*. 2021;25(4):375-383. doi:10.4196/kjpp.2021.25.4.375
- 30. Schroeder DC, Maul AC, Mahabir E, et al. Evaluation of small intestinal damage in a rat model of 6 Minutes cardiac arrest. *BMC Anesthesiol*. 2018;18(1):61. doi:10.1186/s12871-018-0530-8
- 31. Hernández-Cuellar E, Tsuchiya K, Medina-Contreras O, Valle-Ríos R. The Role of Inflammasomes in LPS and Gram-Negative Bacterial Sepsis. *J Clin Med.* 2025;14(19):7102. doi:10.3390/jcm14197102
- 32. buchholz b. m., bauer a. j. Membrane TLR signaling mechanisms in the gastrointestinal tract during sepsis. *Neurogastroenterology & Motility*. 2010;22(3):232-245. doi:10.1111/j.1365-2982.2009.01464.x
- 33. Zhan L, Zheng J, Meng J, Fu D, Pang L, Ji C. Toll-like receptor 4 deficiency alleviates lipopolysaccharide-induced intestinal barrier dysfunction. *Biomedicine & Pharmacotherapy*. 2022;155:113778. doi:10.1016/j.biopha.2022.113778

- 34. Remick DG, Bolgos G, Copeland S, Siddiqui J. Role of Interleukin-6 in Mortality from and Physiologic Response to Sepsis. *Infect Immun*. 2005;73(5):2751-2757. doi:10.1128/IAI.73.5.2751-2757.2005
- 35. Zhao S, Chen F, Yin Q, Wang D, Han W, Zhang Y. Reactive Oxygen Species Interact With NLRP3 Inflammasomes and Are Involved in the Inflammation of Sepsis: From Mechanism to Treatment of Progression. *Front Physiol.* 2020;11. doi:10.3389/fphys.2020.571810
- 36. Zou Z, Liu B, Zeng L, et al. Cx43 Inhibition Attenuates Sepsis-Induced Intestinal Injury via Downregulating ROS Transfer and the Activation of the JNK1/Sirt1/FoxO3a Signaling Pathway. *Mediators Inflamm*. 2019;2019:1-13. doi:10.1155/2019/7854389
- 37. Giridharan V V., Generoso JS, Lence L, et al. A crosstalk between gut and brain in sepsis-induced cognitive decline. *J Neuroinflammation*. 2022;19(1):114. doi:10.1186/s12974-022-02472-4
- 38. Silva CMS, Wanderley CWS, Veras FP, et al. Gasdermin D inhibition prevents multiple organ dysfunction during sepsis by blocking NET formation. *Blood*. 2021;138(25):2702-2713. doi:10.1182/blood.2021011525
- 39. Liu D, Huang SY, Sun JH, et al. Sepsis-induced immunosuppression: mechanisms, diagnosis and current treatment options. *Mil Med Res.* 2022;9(1):56. doi:10.1186/s40779-022-00422-y
- 40. Figueiredo MJ, de Melo Soares D, Martins JM, et al. Febrile response induced by cecal ligation and puncture (CLP) in rats: involvement of prostaglandin E2 and cytokines. *Med Microbiol Immunol*. 2012;201(2):219-229. doi:10.1007/s00430-011-0225-y
- 41. Cauvi DM, Song D, Vazquez DE, et al. Period of Irreversible Therapeutic Intervention during Sepsis Correlates with Phase of Innate Immune Dysfunction. *Journal of Biological Chemistry*. 2012;287(24):19804-19815. doi:10.1074/jbc.M112.359562
- 42. Villa P, Sartor G, Angelini M, et al. Pattern of cytokines and pharmacomodulation in sepsis induced by cecal ligation and puncture compared with that induced by endotoxin. *Clinical Diagnostic Laboratory Immunology*. 1995;2(5):549-553. doi:10.1128/cdli.2.5.549-553.1995
- 43. Vardon Bounes F, Mémier V, Marcaud M, et al. Platelet activation and prothrombotic properties in a mouse model of peritoneal sepsis. *Sci Rep.* 2018;8(1):13536. doi:10.1038/s41598-018-31910-8
- 44. Yoseph BP, Klingensmith NJ, Liang Z, et al. Mechanisms of Intestinal Barrier Dysfunction in Sepsis. *Shock.* 2016;46(1):52-59. doi:10.1097/SHK.000000000000565
- 45. Park YJ, Bae J, Yoo JK, et al. Effects of NF-κB Inhibitor on Sepsis Depend on the Severity and Phase of the Animal Sepsis Model. *J Pers Med.* 2024;14(6):645. doi:10.3390/jpm14060645